



Report

# Estimating hourly population flows in the Netherlands

Statistics Netherlands

December 2020

# Contents

<b>1</b>	<b>Introduction</b>	<b>4</b>
1.1	A different kind of population statistics	4
1.2	Enter mobile phone network data	5
1.3	Data sources used	6
1.4	Methodological outline	7
<b>2</b>	<b>Location estimation</b>	<b>9</b>
2.1	Connection likelihood	9
2.2	Location prior	10
2.3	Signal strength model	11
<b>3</b>	<b>Construction of the flow cube of devices</b>	<b>15</b>
3.1	Estimation of connection fractions	15
3.2	Estimation of a device's place of presence	15
3.3	Estimation of a device's place of residence	16
3.4	Data cleaning	17
3.5	Final assembly of the flow cube	18
<b>4</b>	<b>Construction of the flow cube of persons</b>	<b>19</b>
4.1	Calibration	20
4.2	Example of calibration	21
<b>5</b>	<b>Results</b>	<b>22</b>
5.1	Flow cubes produced	22
5.2	Visualisations of flows	23
<b>6</b>	<b>Summary and outlook</b>	<b>28</b>
6.1	Methodological improvements	28
6.2	Further organisation of methodology	29
	<b>References</b>	<b>30</b>

## Summary

This report contains methodological recommendations for gaining insight hourly population flows. These methodologies were developed during a pilot study by Statistics Netherlands (SN) in collaboration with a Dutch mobile network operator SN. The study used mobile phone network data to map population flows within the Netherlands on an hourly basis over periods of five weeks at the level of municipalities and districts. The estimation and aggregation methods used for constructing these flows are explained and the results that have been obtained so far are summarised. The necessary methods used to protect the privacy of individuals are described as well. In each processing step the amount of detail of the information contained in the network data has been lowered until anonymous outcomes were achieved. No form of tracking of individuals has been implemented.

It is shown that by estimating the presence of people in a given region weekends, working weeks, major football matches, festivals and national holidays can be distinguished. Furthermore, business and commercial regions differ from residential ones by having lower counts on Wednesdays and Fridays and the time of day that the peak of population presence is reached. The relative changes over time of these population estimates hence are rich in information.

## Keywords

Mobile phone, device, signalling data, call detail records, cell, mobile network operator, Bayesian, location, mobility, origin-destination, population flow, inflow, outflow, present population, Municipal Personal Records Database

# 1 Introduction

## 1.1 A different kind of population statistics

One of the most fundamental data sources government agencies in the Netherlands have available about population demographics is the Dutch *Municipal Personal Records Database* (PRD). Every municipality is obliged to register their residents in this database, along with their residential address and other demographic variables. Additionally, many other types of non-residents are (able to have themselves be) logged in the PRD (see [Pri17] for more details). While a faultless register of this type is impossible to create, regular quality monitoring ensures that the PRD is the most reliable and up-to-date source on, in particular, residential population counts.

However, as the complexity of society is increasing, so is the need by public policy makers for more fine-grained and high-dimensional data which could help to understand and address the issues that grow along with this trend. With regards to population counts, value has been found in not merely knowing where people reside, but also to learn their movements over time at a detailed spatial and temporal scale. Statistics on such *population flows* could help to improve urban planning, allocate public and emergency services more effectively, map exposure to environmental pollution and improve epidemic modelling, among other applications. In countries with out-of-date census data, population flows could help to disaggregate and update the census.

Making this idea more concrete: the figures describing such movements can be laid out in a so called *flow cube (of persons)* (sometimes also called an *origin-destination-time matrix* in the literature). It has three axes called *place of residence*, *place of presence* and *time*. The figure contained in the cube at such a triple of coordinates is the number of people present at a given place and time, grouped by their place of residence.

For example, if the smallest resolution of location used is ‘municipality’ and the smallest resolution of time used is ‘hours’, then a selection of rows from the flow cube, presented in a ‘long’ format instead of a ‘wide’ format, could look as in Table 1.1. This table should be read as follows: on 4 December 2020 at 12:00 approximately, 450 people who have municipality A as their municipality of residence were also present in municipality A. At the same time, 50 people whose municipality of residence is municipality A were located in municipality B.

**Table 1.1 An illustration of a selection of rows from a flow cube, presented in a ‘long’ format**

Day	Hour	Place of residence	Place of presence	Count
20201204	12:00	municipality A	municipality A	450
20201204	12:00	municipality A	municipality B	50
20201205	17:00	municipality B	municipality c	650

Traditional surveys, such as the annual national mobility survey [SNd] carried out by Statistics Netherlands (SN), are by themselves not adequate for estimating population flows of this kind. The size of the sample necessary to produce such detailed figures with some level of reliability would prove to be too costly and place an excessive burden on the population. Moreover, surveys are highly reliant on both the respondents’ ability to memorise their daily movements,

and their willingness to keep a detailed log, further increasing difficulties of (high quality) data collection.

## 1.2 Enter mobile phone network data

At this point an introduction of some terminology is in order. To enable telecommunication across a large geographic area, an MNO installs *base stations* at strategically chosen locations. Each base station contains one or more cells, which in turn serve a relatively small area each. These cells, together with the surrounding developed technology and infrastructure, comprise an MNO's (*mobile*) network.

Two types of data are needed from the MNO for statistical inference on the municipality of devices: *cell plan* data, which contains information about the mobile communication network infrastructure, and *event* data. There are generally two types of event data, depending on which transaction events are contained. They do not contain the actual contents of the communication. Event data that are used to calculate the costs in order to bill customers are called *Call Detail Records* (CDR), which contain events related to active mobile phone use<sup>1)</sup>. Event data that also contains passive events such as location updates, are called *signalling data*. These data are used by the MNO for network analysis and optimization. Signalling data are usually much richer than CDR data and are therefore recommended for statistical inference. One can expect a smartphone to generate hundreds of records in a signalling data table per day, of which fewer are generated at night. Besides the active usage by the user, the number of records depends on the brand and operating system of the device and the network technology (2G to 5G) used. Though the pilot research was performed on signalling data, the methodologies presented in this report are applicable to CDR as well. To avoid confusion, we will use the term MNO data henceforth, which can be interpreted as either CDR or signalling data. Any type of MNO data contributes to a more detailed population flow cube.

Its large volume, high spatiotemporal detail and low (additional) cost of collection make for attractive features of MNO data to overcome the limitations of, or supplement traditional registers and surveys. However, even though this data only consists of communication metadata, it can reveal a great amount of information about device's owners. Therefore additional disclosure control measures during data processing are necessary to ensure that their privacy is preserved.

The pilot study allowed SN a unique opportunity to study MNO data within an MNO's data centre, and export anonymised, aggregated datasets to SN's computer infrastructure for further analysis and processing (see [Val+19]). One of the direct goals was to use this data to construct flow cubes of persons for certain observation periods, while a long term ambition of SN is to develop an open and efficient methodology for deriving statistics based on MNO data, which could subsequently be implemented at other MNOS and (national statistical) institutes, both nationally and internationally.

Since the turn of the century many other NSIs, universities and research labs across the globe have started investigating how mobile phone network data can be used to help study human

<sup>1)</sup> CDR data contain records about calls (initiating and receiving), SMS (sending and receiving), and mobile data usage. CDR are collected for billing purposes. Note that in several studies the term CDR is used for data that only contains call and SMS events, and alternative terms *Data Detail Records* (DDR) or *Event Data Records* (EDR) are used for data that also include mobile data usage events.

mobility. We refer to [Che+16] for a reasonably recent overview of the literature. It should be noted, though, that the notions of *origin-destination* and *flow* used in those papers, such as the early, influential [Cal+11], typically do not agree exactly with the type of flow cubes that the current report is focused on.

### 1.3 Data sources used

The primary data source used to construct the flow cubes of persons was a table of 4G MNO data as stored in the big data environment of one of the MNOs of the Netherlands. It should be stressed that this microdata was never transferred to SN – this report explains which datasets were exported to SN, and which disclosure control measures were taken before doing so. No distinction in the processing steps has been made between deliberately and passively generated records. They were treated on equal footing, based on the belief that a larger volume of records, regardless of their type, is likely to lead to better estimates.

Each record in this MNO data table contains over 300 variables. However, for our purposes, only the following three variables were used:

**imsi** standing for International Mobile Subscriber Identity (IMSI), which is an anonymous unique identifier of the device that generated the record. As a measure to protect privacy, neither researchers from the MNO nor from SN have direct access to this identifier, as the actual IMSI is partially hashed to the variable **imsi**,

**start\_time** a time-stamp signifying the start of the interaction of the device with the cell which created the record,

**e\_cgi** a unique identifier of the cell on the MNOs network with which the device interacted.

The rest of the variables may prove to be useful in future research, but understanding their nature will require substantial knowledge of the engineering aspects of the network.

The country of origin of a device can be extracted from the variable **imsi**, since the first three digits of the value of this variable are the country's mobile country code (MCC). This allows one to distinguish in particular records generated by Dutch devices from those generated by roaming devices.

The second data source to be provided by each MNO is an up-to-date *cell plan* of the network, which contains various physical properties and settings of the cells, including their geographical coordinates. The variables that will be used are specified in Section 2.

The third data source is created by SN itself. Based on the PRD, SN periodically publishes figures on the number of residents at several administrative levels, such as municipalities, districts and neighbourhoods. To reduce the risk of disclosure the public figures on districts and neighbourhoods have rounding methods applied to them. We write  $\text{Pop}(x)$  for this publicly available (at [SNc]) number of residents of administrative region  $x$  on 1 January 2017.

The fourth data source to be used is a rectangular grid divided into  $100 \times 100$  metres square tiles which covers the Netherlands, including the Wadden Sea, the West Frisian Islands and a 25 kilometres offshore coastal zone. Specifically, the grid uses the map projection known as 'Amersfoort / RD new', denoted by EPSG:28992.

The fifth data source was the digital geometry of the boundaries of all municipalities, districts and neighbourhoods in the Netherlands in 2017, as created by SN. This resource is publicly available as well at [SNe] in the Esri shapefile format.

The sixth data source consists of a *Current Dutch Elevation* file, which is a digital elevation map of the Netherlands. More precisely, the version of this map available at [PDOK] for  $25 \times 25$  metres square tiles will be used. Its construction is the result of a collaboration between the Dutch provinces, government and water boards.

## 1.4 Methodological outline

The processing pipeline which constructs flow cubes of persons starts with a Bayesian model which, given a connection of a device to a cell, estimates the geographic location of the device. The model considers each connection of a device individually. Likelihoods of presence in a municipality are calculated independently of all other connections of both the device and the cell. The model only uses the cell plan, the grid and the boundaries of administrative regions, as described in Section 1.3, as input data, and it does not make use of the MNO data. Therefore we consider this model as the *static* component of the pipeline. The output of the static component is a table with probabilities of presence in municipalities given a connection to a cell. It is explained in Section 2.

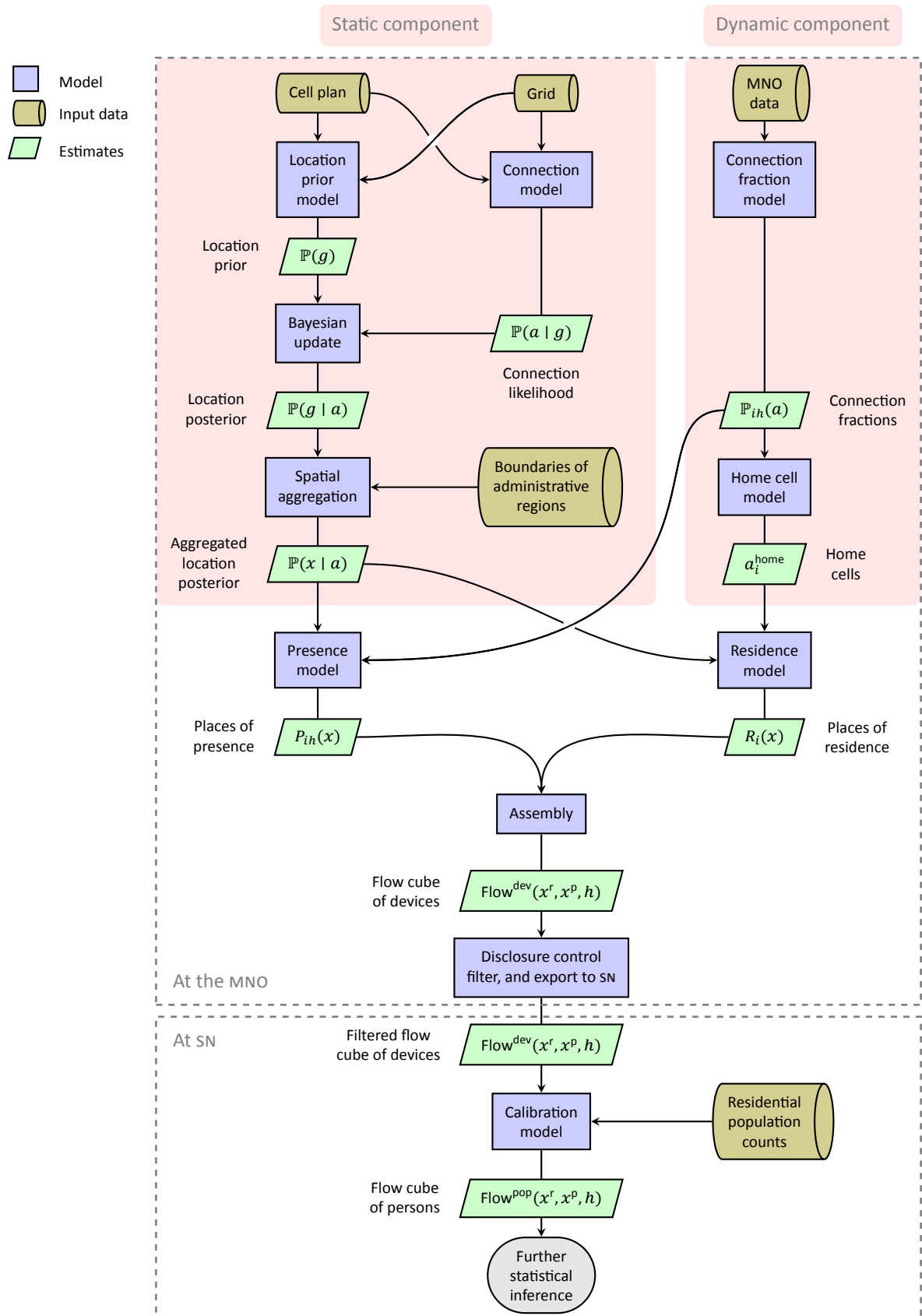
Independently of this static component a *dynamic* component is the only place in the pipeline where the MNO data is used. It estimates for every Dutch device and cell present in the MNO data, and every hour in the chosen observation period of 30 days the fraction of the hour the device spent connected to the cell. These fractions are then used to estimate for every Dutch device its *home cell*, meaning (roughly) the cell to which it connected to the longest. The output of the dynamic component is a table with connection fractions of devices and cells. This dynamic component is explained in Sections 3.1, 3.3 and 3.4.

After studying Section 2 and the aforementioned parts of Section 3 the reader might find it helpful to return to Figure 1.1 to see how the various methods fit together.

The next step in the processing pipeline is the combination of the outputs of the static and dynamic components to estimate for every device in the MNO data probable places of residence and, for each hour, probable places of presence. (Here, the place of residence of a device refers to that of its owner.) These place estimates are then assembled into a *flow cube of devices*, which has the same axes as a flow cube of persons, but the figures now represent estimates of numbers of Dutch devices on the network of the MNO making use of 4G technology.

All processing steps explained so far took place inside the secured computer infrastructure of the MNO. Before exporting the constructed flow cube of devices to SN a disclosure preventing filtering procedure is applied to it. The resulting filtered cube is finally *calibrated* into a flow cube of persons at SN, using the residential population counts based on the PRD. These steps are further explained in Sections 3.2, 3.3, 3.5 and 4. After studying those Sections the reader can return to Figure 1.1 for a visual summary. It should be noted that all methods involved naturally estimate numbers of devices or people as decimal numbers, instead of as integers, unlike the column 'count' in the example of Table 1.1 suggests.

Figure 1.1 The processing pipeline



## 2 Location estimation

Recall that two of the dimensions of a flow cube are spatial: place of residence and place of presence. However, a raw MNO data table contains no GPS data or demographic data on the owner of the device. An MNO has some demographic data on its customers – at least their name and postal address – but it is only allowed to join these with MNO data for the purpose of billing. Moreover, postal addresses of phones for business usage are frequently business addresses, and must therefore be considered unreliable. Constructing a flow cube of devices therefore requires one to approximate these places instead.

For this purpose a Bayesian model was developed which estimates the probability  $\mathbb{P}(g \mid a)$  that a device is present in a grid tile  $g$  given its connection to some cell  $a$ . We have in particular that summing over all tiles  $g$  gives  $\sum_g \mathbb{P}(g \mid a) = 1$ , which reflects that a device (when connected to a cell) is located with probability 1 somewhere within the MNOS network range. As our notation of this probability already suggests, the model does not use or assume any information about the device, except that it is connected to  $a$ .

Our location estimation model uses Bayes' formula in the following way:

$$\mathbb{P}(g \mid a) \propto \mathbb{P}(a \mid g)\mathbb{P}(g). \quad (1)$$

The *connection likelihood*  $\mathbb{P}(a \mid g)$  is the probability that a device is connected to cell  $a$  given that the device is located in grid tile  $g$ . The probability  $\mathbb{P}(g)$  that a device is located in  $g$  without any connection knowledge represents the *location prior* about the relative frequency of connections made from  $g$ . Together they allow the calculation of  $\mathbb{P}(g \mid a)$ , which will henceforth be referred to as the *location posterior*.

The places of presence and residence of devices will be calculated at a coarser spatial level than that of grid tiles, namely in terms of neighbourhoods, districts and municipalities. The translation to such an administrative region  $x$  is done by defining the *aggregated location posterior* as

$$\mathbb{P}(x \mid a) := \sum_{g \in x} \mathbb{P}(g \mid a), \quad (2)$$

where we write  $g \in x$  if the center of  $g$  lies in  $x$ . The reason to use the intermediary grid tiles is to allow for a more detailed modelling of location priors and connection likelihoods.

The rest of this section explains the models used for the location prior and connection likelihood. Further elaborations on, and extensions of the location estimation model can be found in [TGS20].

### 2.1 Connection likelihood

We model the connection likelihood  $\mathbb{P}(a \mid g)$  as

$$\mathbb{P}(a \mid g) := \frac{s(g, a)}{\sum_{a' \in \mathcal{A}} s(g, a')}, \quad (3)$$

where  $\mathcal{A}$  is the set of all cells in the MNOS network and  $s(g, a) \in [0, \infty)$  stands for the *signal dominance* (an umbrella term introduced by ourselves) received in grid tile  $g$  from cell  $a$ . That

is, the connection likelihood is the ratio of the signal dominance received from  $a$  to the total value of signal dominance received from all cells. Different choices for modelling the signal dominance are possible, and any choice defines the *connection model* in Figure 1.1. Note that  $\mathbb{P}(a | g)$  is independent of rescaling the function  $s(g, a)$  by a constant factor, and our convention is that  $s(g, a)$  should be defined so as to take on values in the interval  $[0, 1]$ . In Section 2.3 we propose a definition of the connection model by first approximating the signal strength  $S(g, a)$  measured in dBm, followed by a transformation to obtain a signal dominance  $s_{\text{strength}}(g, a)$ . That is, this signal dominance will be an expression in terms of the approximated signal strength.

## 2.2 Location prior

Any model of the location prior will make assumptions on where devices are expected to be. In this section two options are discussed: the uniform prior and the network prior. More advanced models are presented in [TGS20].

Write  $\mathcal{G}$  for the set of all tiles in the grid. When we use the *uniform prior*, we assume the probability of a device being in any grid tile is the same value for every tile:

$$\mathbb{P}_{\text{uniform}}(g) := \frac{1}{|\mathcal{G}|}. \quad (4)$$

In Bayesian statistics a uniform prior is sometimes viewed as uninformative. In the case of mobile phone data, however, the implicit assumption that any grid tile is as likely as the next can lead to an underestimation of devices in urban areas and an overestimation of devices in rural areas. We therefore advise against using the uniform prior as a default prior without consciously assessing the plausibility of the underlying assumption.

A *network prior* is defined as follows in terms of any choice for a model  $s(g, a)$  for the signal dominance:

$$\mathbb{P}(g) := \frac{\sum_{a \in \mathcal{A}} s(g, a)}{\sum_{a \in \mathcal{A}} \sum_{g' \in \mathcal{G}} s(g', a)}. \quad (5)$$

This prior, together with the model (3) for the connection likelihood  $\mathbb{P}(a | g)$  simplifies eq. (1) to

$$\mathbb{P}(g | a) \propto s(g, a). \quad (6)$$

The interpretation of the prior (5) depends on the instance of the signal dominance  $s(g, a)$  one has chosen. If the instance  $s_{\text{strength}}(g, a)$ , to be introduced in Section 2.3 is used, we will speak of *the network prior* and denote it by  $\mathbb{P}_{\text{strength}}(g)$ . Basically,  $\mathbb{P}_{\text{strength}}(g)$  reflects the distribution of the total signal over the entire grid. This prior contains implicit knowledge about where an MNO is expecting people. The placement of cells namely is not without reason; generally, more cells are placed in crowded areas, such as city centers, than in quiet rural areas. Note that we could have defined the network prior using the cell density. However, since the network capacity also depends on the type and configuration of the cells and on the environment (buildings and trees will generally have a negative effect on the propagation) we use the signal dominance, in which these aspects are taken into account.

There are two aspects to be aware of when using the network prior. First, the placement of cells is based on estimated peak traffic rather than the average expected number of devices.

Usually, MNOS provide better network coverage in railway stations than in residential areas, since the estimated peak traffic is higher; people typically use their phone more actively in railway stations and moreover, the expected number of devices fluctuates more over time. The second aspect to keep in mind is that MNOS also may place extra overlapping cells in order to provide network coverage for specific patches of land, which implies that some parts of land with already good coverage will have an improved network coverage, whereas the expected number of devices does not change. In summary, the total signal strength of the network does not always reflect the estimated number of devices.

## 2.3 Signal strength model

This section describes the propagation of signal strength originating from a single cell. We distinguish two types of cells: omnidirectional and directional, resulting in two different propagation models. Omnidirectional cells have no aimed beam and their coverage area can be thought of as a circular disk. Directional cells point in a certain direction and their coverage area can be thought of as an oval with one axis of symmetry. In practice, small cells are omnidirectional and normal cells (i.e. attached to cell towers or placed on rooftops) are directional [Kor+16].

### 2.3.1 Omnidirectional cells

For omnidirectional cells, propagation of the signal strength  $S(g, a)$  is modelled as

$$S(g, a) := S_0 - S_{\text{dist}}(r_{g,a}), \quad (7)$$

where  $S_0$  is the signal strength at  $r_0 = 1$  meter distance from the cell in dBm and  $r_{g,a}$  is the distance between the center of grid tile  $g$  and cell  $a$  in meters (we take into account the placement height of the cell, but assume that devices are situated at ground level). The value of  $S_0$  can be different for every cell and is assumed to be a known property. In cell plan information, it is common to list the power  $P$  of a cell in Watt, rather than the signal strength in dBm. The value of  $S_0$  can be calculated from  $P$  using the conversion between Watt and dBm [FF10]:

$$S_0 = 30 + 10 \log_{10}(P). \quad (8)$$

The function  $S_{\text{dist}}(r)$  returns the loss of signal strength as a function of distance  $r$ :

$$S_{\text{dist}}(r) := 10 \log_{10}(r^\gamma) = 10\gamma \log_{10}(r), \quad (9)$$

where  $\gamma$  is the *path loss exponent*, which resembles the reduction of propagation due to reflection, diffraction and scattering caused by objects such as buildings and trees [SH09]. In free space,  $\gamma$  equals 2, which is what we used, but varying values would result in a more physically accurate model. Methods to vary the path loss exponent using land use data are explored in [TGS20].

### 2.3.2 Directional cells

A directional cell is a cell that is aimed at a specific angle. Along this angle, the signal strength is received at its best. However, the signal can also be strong in other directions. It is comparable to a speaker producing sound in a specific direction. The sound is audible in many directions, but is much weaker at the sides and the back of the speaker. We specify the beam of a directional cell  $a$  by four parameters:

- The azimuth angle  $\varphi_a$  is the angle from the top view between the north and the direction in which the cell is pointed, such that  $\varphi_a \in [0, 360)$  degrees. Note that cell towers and rooftop cells often contain three cells with 120 degrees in between.
- The elevation angle  $\theta_a$  is the angle between the horizon plane and the tilt of the cell. Note that this angle is often very small, typically only four degrees. The plane that is tilt along this angle is called the *elevation plane*.
- The horizontal beam width  $\alpha_a$  specifies in which angular difference from the azimuth angle in the elevation plane the signal loss is 3 dB or less. At 3 dB, the power of the signal is halved. The angles in the elevation plane for which the signal loss is 3 dB correspond to  $\varphi_a \pm \alpha_a/2$ . In practice, these angles are around 65 degrees.
- The vertical beam width  $\beta_a$  specifies the angular difference from  $\theta_a$  in the vertical plane orthogonal to  $\varphi_a$  in which the signal loss is 3 dB. The angles in which the signal loss is 3 dB correspond to  $\theta_a \pm \beta_a/2$ . In practice, these angles are around 9 degrees.

Let  $\delta_{g,a}$  be the angle in the elevation plane between the azimuth angle  $\varphi_a$  and the orthogonal projection on the elevation plane of the line between the center of cell  $a$  and the center of grid tile  $g$ . Similarly, let  $\varepsilon_{g,a}$  be the angle from the side view between the line along the elevation angle  $\theta_a$  and the line between the center of cell  $a$  and the center of grid tile  $g$ . Note that  $\varepsilon_{g,a}$  depends on the cell property of the installation height above ground level. We model the signal strength for directional cells as

$$S(g, a) := S_0 - S_{\text{dist}}(r_{g,a}) - S_{\text{azi}}(\delta_{g,a}, \alpha_a) - S_{\text{elev}}(\varepsilon_{g,a}, \beta_a), \quad (10)$$

where  $S_0$  is the signal strength at  $r_0 = 1$  meter distance from the cell, in the direction of the beam so that  $\delta = 0$  and  $\varepsilon = 0$ . The signal loss due to distance to the cell, azimuth angle difference and elevation angle difference is specified by  $S_{\text{dist}}$ ,  $S_{\text{azi}}$  and  $S_{\text{elev}}$ , respectively. The definition of  $S_{\text{dist}}$  is similar to the omnidirectional cell and can be found in eq. (9).

Each cell type has its own signal strength pattern for both the azimuth and elevation angles. These patterns define the relation between signal loss and the offset angles, i.e.,  $\delta_{g,a}$  for the azimuth and  $\varepsilon_{g,a}$  for the elevation angles. We model the radiation pattern for both  $S_{\text{azi}}$  and  $S_{\text{elev}}$  by a linear transformation of the Gaussian formula, each with different values for parameters  $c$  and  $\sigma$ . Let

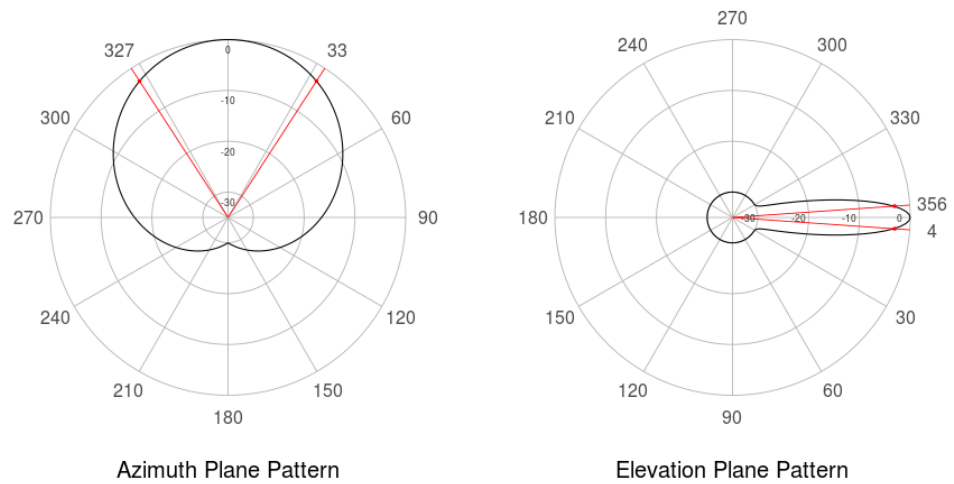
$$f(\varphi) := c - c \exp\left(-\frac{\varphi^2}{2\sigma^2}\right), \quad (11)$$

where  $c$  and  $\sigma^2$  are constants, whose value is determined by numerically solving equations for a set of constraints. These constraints are different for  $S_{\text{azi}}$  and  $S_{\text{elev}}$  and depend on cell properties.

The resulting patterns are shown in Figure 2.1. The black line shows the relation between signal loss and angle in the azimuth plane (left) and elevation plane (right). The grey circles correspond to the signal loss; the outer circle means 0 dB loss (which is only achieved in the main direction), the next circle corresponds to 5 dB loss, and so forth. The red lines denote the angles corresponding to 3 dB loss. The angle between the red lines is  $2\alpha_a$  in the azimuth plane and  $2\beta_a$  in the elevation plane. Although these models approximate the general curve of real radiation patterns, the radiation patterns are more complex in reality, e.g. they often contain local spikes caused by so-called side and back lobes.

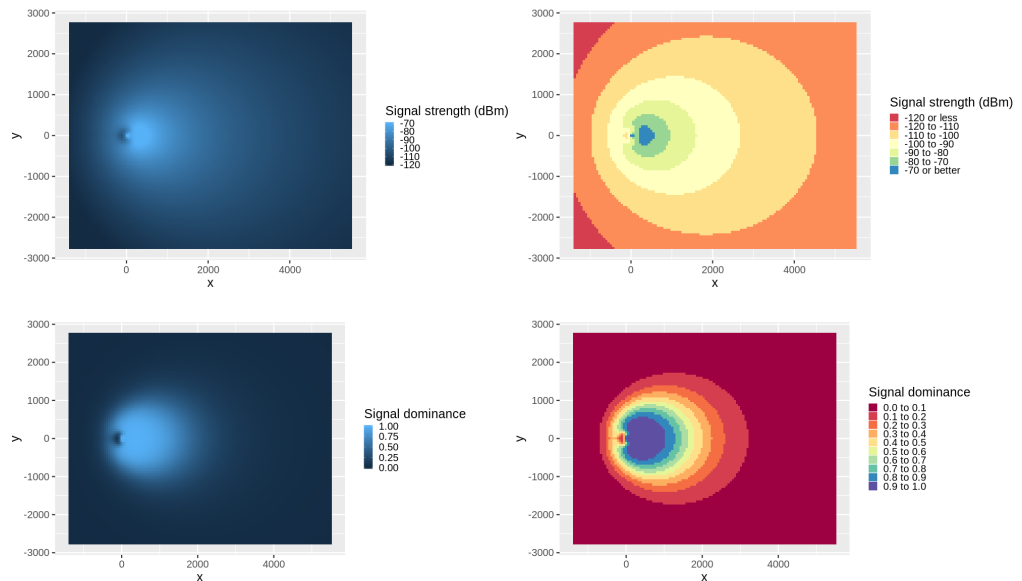
Figure 2.2 (top row) illustrates the signal strength at the ground level from above for a specific cell. In this case, the cell is placed at  $x = 0, y = 0$  at 55 meters above ground level in an urban

**Figure 2.1 Radiation patterns for the azimuth and elevation planes**



environment ( $\gamma = 4$ ), has a power of 10 W, and is directed eastwards with an elevation angle (tilt) of 5 degrees, a horizontal beam width of 65 degrees and a vertical beam width of 9 degrees. Notice that the signal strength close to the cell, which on ground level translates to almost under the cell, is lower than at a couple of hundred meters distance. This is caused by relatively large  $\epsilon$  angles at grid tiles nearby the cell.

**Figure 2.2 Signal strength (top row) and signal dominance (bottom row) at ground level**

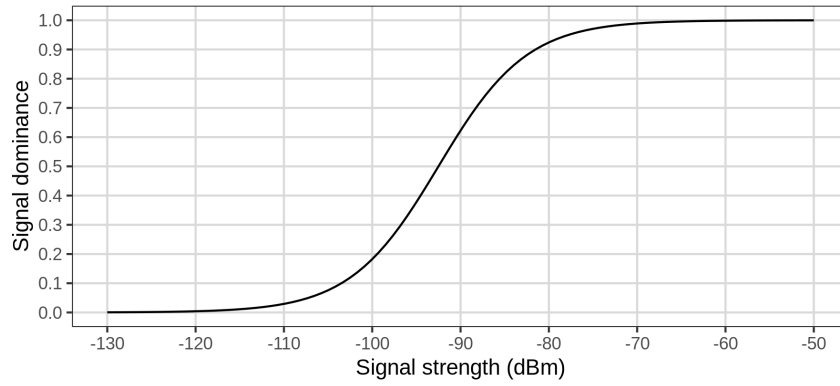


### 2.3.3 Signal dominance

The assignment of a cell to a mobile device does not only depend on received signal strength, but also on the capacity of the cells. The process of assigning devices to cells while taking into account the capacity of the cells is also called *load balancing*.

Our model allows for two phenomena that we feel should not be overlooked. The first is the switching of a device when it is receiving a bad signal to a cell with a better signal. Table 2.1

**Figure 2.3 Logistic relation between signal strength and signal dominance**



describes how the signal strength can be interpreted in terms of quality for 4G networks [Kor+16]. The second phenomenon is the switching between cells that is influenced by some decision making system in the network that tries to optimize the load balancing within the network. The specifics of this system are considered unknown.

**Table 2.1 Indication of quality for signal strength in 4G networks**

Signal strength (dBm)	Quality
−70 or higher	Excellent
−90 to −70	Good
−100 to −90	Fair
−110 to −100	Poor
−110 or less	Bad or no signal

We assume that a better signal leads to a higher chance of connection. When a device has multiple cells available with a signal strength above a certain threshold, say −90 dBm, the signal strengths are both more than good enough and the cell with the highest capacity is selected rather than the cell with the best signal strength. When the choice is between cells with a lower signal strength, one can imagine that their relative differences play a more important role in the connection process. However, when there are multiple cells available with a poor signal strength, it can be assumed that the signal strength value is less important than having capacity. In short, we assume that signal strength plays a more important role in load balancing when it is in the middle range instead of in the high quality or low quality ranges.

To model this take on the load balancing mechanism, we use a logistic function to translate the signal strength  $S(g, a)$  to the more interpretable signal dominance measure  $s_{\text{strength}}(g, a)$ , which is then used to define the connection likelihood (3). Let us define

$$s_{\text{strength}}(g, a) := \frac{1}{1 + \exp(-S_{\text{steep}}(S(g, a) - S_{\text{mid}}))}, \quad (12)$$

where  $S_{\text{mid}}$  and  $S_{\text{steep}}$  are parameters that define the midpoint and the steepness of the curve respectively. Figure 2.3 shows an example of eq. (12). In that Figure  $S_{\text{mid}}$  and  $S_{\text{steep}}$  are set to −92.5 dBm and 0.2 dBm respectively to resemble Table 2.1. The signal dominance at ground level is shown in Figure 2.2 (bottom row). The values that are shown are normalized by the sum of all values over all grid tiles, such that the normalized values form a probability distribution. Compared to the signal strength shown in Figure 2.2 (top row), the signal dominance puts more emphasis on the geographic area that is in the range of the cell. Whether these signal dominance values resemble reality, should be validated by field tests.

# 3 Construction of the flow cube of devices

This Section starts by describing how the MNO data is used to estimate connection fractions of observed devices. Together with a location posterior computed in Section 2 these fractions serve as the input data for models which estimate places of presence (Section 3.2) and residence (Section 3.3) for all devices present in the MNO data. The assembly of these estimated places into a flow cube of devices is explained in Section 3.5, along with the privacy-protecting filtering procedure to make the cube suitable for export to SN.

## 3.1 Estimation of connection fractions

A device can make more than one connection per hour, even with the same cell. The number of connections per hour can moreover vary strongly between devices and different hours. Since we want to estimate population flows on an hourly basis, it is necessary to account in various computations for this phenomenon. More precisely: given a device  $i$  and an hour  $h$ , the estimated fraction of  $h$  that  $i$  spent connected to a cell  $a$  is an important value. We denote this fraction by  $\mathbb{P}_{ih}(a)$  to suggest an alternative interpretation: it is the probability that  $i$  connected to  $a$  during  $h$ . It is estimated from the MNO data by

$$\mathbb{P}_{ih}(a) := \frac{\#\{\text{connections made by } i \text{ at } a \text{ during } h\}}{\#\{\text{connections made by } i \text{ during } h\}}. \quad (13)$$

If  $i$  made no connections during  $h$  then we define  $\mathbb{P}_{ih}(a)$  to be 0. If  $i$  made at least one connection during  $h$ , then  $\sum_a \mathbb{P}_{ih}(a) = 1$ .

## 3.2 Estimation of a device's place of presence

To estimate the place of presence the probability distribution of the device  $i$  at hour  $h$  is defined as

$$P_{ih}(x) := \sum_a \mathbb{P}_{ih}(a) \cdot \mathbb{P}(x | a), \quad (14)$$

where  $x$  stands for an arbitrary administrative region and  $\mathbb{P}(x | a)$  is a location posterior as defined in Section 2. If  $i$  made no connections during  $h$  then  $\sum_x P_{ih}(x) = 0$ . If  $i$  made at least one connection during  $h$ , then obviously  $\sum_x P_{ih}(x) = 1$ .

The definition of eq. (14) can be motivated as follows. We first approximate the fraction  $P_{ih}(x)$  of  $h$  that  $i$  spent in  $x$  by

$$P_{ih}(x) \approx \frac{\#\{\text{connections made by } i \text{ from } x \text{ during } h\}}{\#\{\text{connections made by } i \text{ during } h\}}. \quad (15)$$

This is of course a coarse approximation since it does not take the timestamps of the connections during  $h$  into account. In any case, we next bring cells into the picture by noting that the set in the numerator in eq. (15) is a disjoint union over all cells in the MNO's network:

$$\begin{aligned} & \{\text{connections made by } i \text{ from } x \text{ during } h\} \\ &= \bigsqcup_a \{\text{connections made by } i \text{ from } x \text{ at } a \text{ during } h\}. \end{aligned} \quad (16)$$

Therefore, eq. (15) can be expanded to

$$P_{ih}(x) \approx \sum_a \frac{\#\{\text{connections made by } i \text{ from } x \text{ at } a \text{ during } h\}}{\#\{\text{connections made by } i \text{ during } h\}}. \quad (17)$$

The MNO data tells us how often  $i$  made an connection at a cell  $a$  during  $h$ , and given each such connection there is a probability  $\mathbb{P}(x | a)$  that the connection was made from  $x$ . Hence, the numerator in each term in (17) can be estimated as

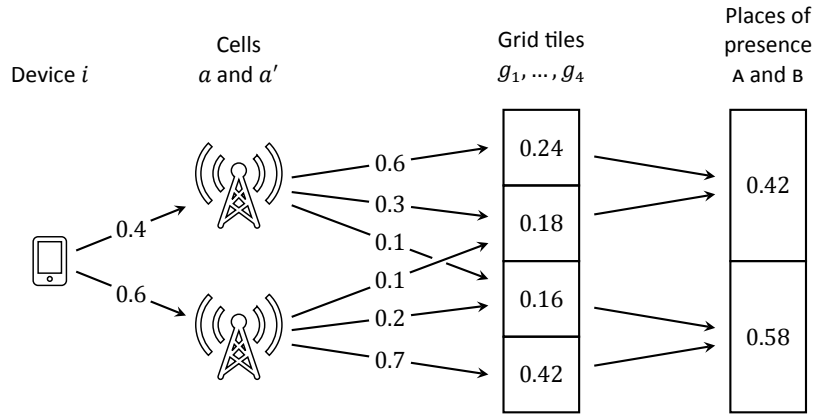
$$\begin{aligned} &\#\{\text{connections made by } i \text{ from } x \text{ at } a \text{ during } h\} \\ &\approx \#\{\text{connections made by } i \text{ at } a \text{ during } h\} \cdot \mathbb{P}(x | a), \end{aligned} \quad (18)$$

with which we arrive at the right-hand side of eq. (14).

Let us give an illustration of this model. Fix a device  $i$  and an hour  $h$ . Assume that the MNO's network consists of two cells  $a$  and  $a'$  and that the Netherlands is partitioned into four grid tiles  $g_1, \dots, g_4$ , of which  $g_1$  and  $g_2$  together form a region A, while B is the union of  $g_3$  and  $g_4$ . The tiles  $g_1, g_2$  and  $g_3$  fall within the range of  $a$ , and  $g_2, g_3$  and  $g_4$  form the range of  $a'$ . All these objects are shown in Figure 3.1, ordered from top to bottom. The figures on the arrows from the cells to the grid tiles are examples of location posterior distributions.

Suppose that  $i$  connected to both  $a$  and  $a'$  during  $h$ , and that it follows from the MNO data that  $P_{ih}(a) = 0.4$  and  $P_{ih}(a') = 0.6$ . The estimated probabilities for the municipality of presence during  $h$  across the grid tiles are then shown in the third column of Figure 3.1, while the fourth column lists the aggregated probabilities across the regions A and B.

**Figure 3.1 Illustration of the estimation of places of presence**



### 3.3 Estimation of a device's place of residence

To estimate the place of residence of a device  $i$  its *home cell*  $a_i^{\text{home}}$  was determined first, meaning (roughly) the cell to which  $i$  was connected to the longest during the observation period of 30 days. One might determine this starting by calculating for each cell the total number of hours connected to it by  $i$  over the entire period, then sorting the cells by these hour totals and finally selecting the top ranked. Due to some computational barriers, this process was implemented slightly differently, as explained next.

First, for each cell  $a$  the number of hours  $h_{iw}^{\text{tot}}(a)$  connected to it by the device  $i$  was calculated per subperiod of a number of days, depending on the available computational capacities and the size of the selected data. For simplicity's sake, let us look at an example where this period

consists of 7 days so the number of connected hours is calculated per separate week  $w$ . This was done by summing the connection fractions  $\mathbb{P}_{ih}(a)$  associated to all hours in that week:

$$h_{iw}^{\text{tot}}(a) := \sum_{h \in w} \mathbb{P}_{ih}(a) \quad (\text{a sum over } 24 \cdot 7 \text{ hours}). \quad (19)$$

To reduce the amount of memory needed to store all these hour counts, for each device only the top ten cells per week (in terms of connected hours) were preserved. The datasets per week were then combined into a single dataset by summing the number of hours per device and cell over all weeks in the observation period:

$$h_i^{\text{tot}}(a) := \sum_w h_{iw}^{\text{tot}}(a) \quad (\text{a sum over 30 days}). \quad (20)$$

It is assumed that the top ten per week will always include the cell the device connected to the most amount of hours during the 30 day period. Finally, the home cell  $a_i^{\text{home}}$  of device  $i$  is set to be the cell which maximises the number of hours  $h^{\text{tot}}(i, a)$ :

$$a_i^{\text{home}} := \arg \max_a h_i^{\text{tot}}(a) \quad (\text{the top ranked of combined non-unique cells}). \quad (21)$$

Given this home cell, the probability that the device  $i$  has a region  $x$  as its place of residence is determined using the aggregated location posterior distribution:

$$R_i(x) := \mathbb{P}(x \mid a_i^{\text{home}}). \quad (22)$$

Note that  $R_i$  is a probability mass function because  $\mathbb{P}(\cdot \mid a_i^{\text{home}})$  is: summing over all regions  $x$  gives  $\sum_x R_i(x) = 1$ , which reflects that a device which has a home cell must have its municipality of residence somewhere within the MNO's network range. Technically, all non-Dutch regions (such as Belgium or Germany) must be viewed as one big region for  $\sum_x R_i(x) = 1$  to hold. From this step, a place of residence will remain per device for the observation period. All other intermediate data, such as lists of top 10 cell connections are no longer needed and were not saved.

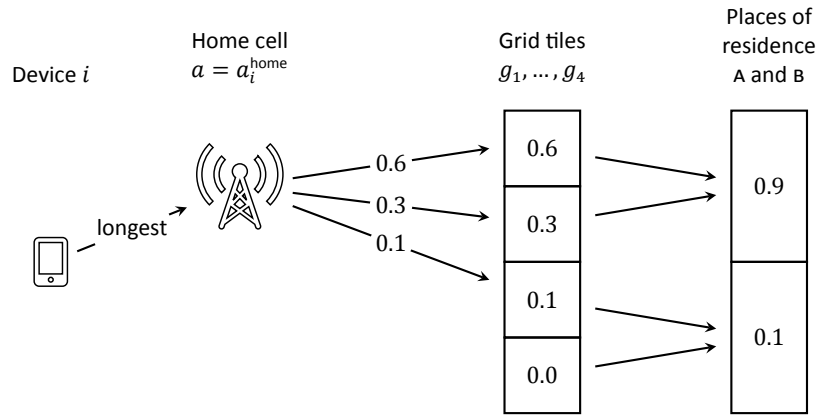
An alternative approach might be to consider the most frequently connected cell at nighttime. The advantage of the proposed approach, however, is that it does not need a definition of 'nighttime' and therefore is unlikely to be biased against people with unusual night and day mobility patterns. A disadvantage, though, is that the devices of people who spend more time near their place of work than usual for the average fulltime job, possibly due to long working days or social activities, may receive an incorrect approximation of their place of residence.

An illustration of this model might again be helpful. We continue the example given in Section 3.2, and suppose that the home cell  $a_i^{\text{home}}$  of the device  $i$  has been determined to be the cell  $a$ . The estimated probabilities for the place of residence across the grid tiles are then shown in the third column of Figure 3.2, while the fourth column lists the aggregated probabilities across the regions A and B.

### 3.4 Data cleaning

The relation between observed devices and a flow cube of persons is not one-to-one. During the data cleaning step, the MNOs are expected to investigate and report on inconsistencies. This will contribute to a more realistic unison of data from the different MNOs.

**Figure 3.2 Illustration of the estimation of places of residence**



For example, the method explained in Section 3.3 assigns to every device a home cell and hence a mass function of probable places of residence. However, it was found that the distribution across all Dutch devices of the fraction of the observation period that devices spent connected to their home cell was bimodal. The two peaks were best separated by dividing this distribution at 60 hours of connection. About 25% of all devices present in the MNO data then connected to their home cell for less than 60 hours during the observation period. The probable municipalities of residence derived from such a cell are considered unlikely to be near the true municipality of residence of the device's owner. We have dubbed these devices *wandering devices* and have not studied them further and decided to discard them before further processing. From this point onwards in this document 'all devices' will stand for only those which crossed the threshold of hours. When this threshold is determined, the length of the observation period should be taken into account.

### 3.5 Final assembly of the flow cube

Having estimates of a device's place of residence and, at every hour, place of presence now gives all the components to build the following 2-dimensional matrix of device  $i$  for hour  $h$ :

$$RP_{ih}(x^r, x^p) := R_i(x^r) \cdot P_{ih}(x^p). \quad (23)$$

It stores the probability that  $i$  has place of residence  $x^r$  (which is independent of  $h$ ) and place of presence  $x^p$  during hour  $h$ . The multiplication in the above equation is based on the assumption that the probability mass functions of place of residence  $R_i$  and place of presence  $P_{ih}$  are independent from each other. If  $i$  made at least one connection during  $h$ , then  $RP_{ih}$  is a joint probability mass function: we have

$$\sum_{x^r} \sum_{x^p} RP_{ih}(x^r, x^p) = 1. \quad (24)$$

If  $i$  made no connections during  $h$ , then the above double sum equals 0.

At face value the assumption of independence might seem erroneous: surely knowledge of a device's place of residence should affect the probability of the place of presence? Our justification is based on interpreting  $R_i$  and  $P_{ih}$  as mass functions *conditioned on the MNO data of  $i$  during the observation period*. That is, it is assumed to be known what the home cell of  $i$  and the cells connected to during  $h$  are. Given this information, the functions  $R_i$  and  $P_{ih}$  are not spread out over the entirety of the Netherlands any longer, but are in practice each

concentrated in a small number of regions. Our assumption is hence more precisely stated as independence of these two conditional probability mass functions. This implicit knowledge of the MNO data has been left out of notations for the sake of brevity.

Continuing the illustrations given in Sections 3.2 and 3.3, the result of the calculation of the matrix  $RP_{ih}$  is shown in Figure 3.3.

**Figure 3.3 Illustration of the assembly of places of presence and residence**

		Municipality of presence	
		A	B
		0.42	0.58
Municipality of residence	A	0.9	0.1
	B	0.378	0.522
		0.042	0.058

The total flow cube of devices  $\text{Flow}^{\text{dev}}$  is obtained by summing all matrices  $RP_{ih}(x^r, x^p)$  over all devices  $i$  for each hour  $h$ :

$$\text{Flow}^{\text{dev}}(x^r, x^p, h) := \sum_i RP_{ih}(x^r, x^p). \quad (25)$$

All processing steps explained so far took place securely at the MNO. Even though the MNO data now only consists of the total number of devices counted per municipality, and does not contain any individual record, to further reduce a possible risk of disclosure the figures in the flow cube of devices strictly lower than 15 were deleted. The resulting filtered cube was then exported to SN.

At this point the cube can be used to estimate the *incoming* and *outgoing flow* of devices for a given region  $x$  and hour  $h$ . By this we mean the number of devices entering or leaving  $x$  from other places, possibly including  $x$  itself. They are computed respectively as follows:

$$\text{Flow}_{\text{in}}^{\text{dev}}(x, h) := \sum_{x^r} \text{Flow}^{\text{dev}}(x^r, x, h), \quad (26)$$

$$\text{Flow}_{\text{out}}^{\text{dev}}(x, h) := \sum_{x^p} \text{Flow}^{\text{dev}}(x, x^p, h). \quad (27)$$

In other words, the inflow is calculated by summing over all places of residence, while the outflow is calculated by summing over all places of presence.

## 4 Construction of the flow cube of persons

The elements of the flow cube  $\text{Flow}^{\text{dev}}$  of devices are estimates of numbers of devices. These figures differ from the corresponding numbers of persons for at least the following reasons:

- They represent merely counts of devices of the MNO from which the MNO data is obtained. The people who communicate via different MNOS are therefore excluded.
- Not everyone owns a mobile phone, or if they do, carry their devices everywhere with them. This holds especially for young children and the elderly.
- Some people might carry multiple devices with them. One can think of, for example, people carrying both a phone for work and one for personal use.

The cube of devices hence needs to be transformed or *calibrated* to a flow cube  $\text{Flow}^{\text{pop}}$  of persons (with axes and dimensions equal to those of  $\text{Flow}^{\text{dev}}$ ). Before proceeding to the description of the calibration method, note that from such a cube incoming and outgoing flows of persons can be calculated in the exact same way as from the flow cube of devices. They are denoted by  $\text{Flow}_{\text{in}}^{\text{pop}}(x, h)$  and  $\text{Flow}_{\text{out}}^{\text{pop}}(x, h)$ , respectively, for every region  $x$  and hour  $h$ .

## 4.1 Calibration

Recall from Section 1.3 the definition of the residential population figures  $\text{Pop}(\cdot)$ , based on the PRD. Our calibration method was based on the assumption that the flow cube  $\text{Flow}^{\text{pop}}$  of persons ought to satisfy the following combination of two equations for all places  $x^r$  and  $x^p$  and hours  $h$ :

$$\frac{\text{Flow}_{\text{out}}^{\text{pop}}(x^r, x^p, h)}{\text{Flow}_{\text{out}}^{\text{pop}}(x^r, h)} = \frac{\text{Flow}^{\text{dev}}(x^r, x^p, h)}{\text{Flow}_{\text{out}}^{\text{dev}}(x^r, h)}, \quad (28a)$$

$$\text{Flow}_{\text{out}}^{\text{pop}}(x^r, h) = \text{Pop}(x^r). \quad (28b)$$

If we momentarily leave out the reference to the hour  $h$  for brevity, eq. (28a) can be understood as the following claim:

Suppose that a certain fraction of the residents of  $x^r$  is present in  $x^p$ . Then the same fraction of the MNOS devices with place of residence  $x^r$  is also present in  $x^p$ . The converse implication holds as well.

In other words, the first equation assumes a uniform presence of the MNOS devices in the flow of persons from location  $x^r$ . This homogeneity is not obvious, because, for example, the market share of the MNO in the flow from  $x^r$  to a location  $x_1^p$  might differ from that in the flow to another location  $x_2^p$ . Further research is needed to quantify the bias resulting from this assumption.

The second equation (28b) results from the assumption

The number of residents of  $x^r$  who are present in any of the regions  $x$  considered together equals the number of residents of  $x^r$ .

This assumption of course introduces a small error since the date (in our case 1 January 2017) for which the figure  $\text{Pop}(x^r)$  was determined is somewhat different from the observation period for which the MNO data was obtained. A larger error is introduced if the set of regions  $\{x\}$  does not also include locations abroad. Residents of  $x^r$  might namely be abroad during (part of) the observation period. Correcting for this misestimation would involve additional tourism or holiday statistics, which we did not attempt at this stage of the project. The assumption used hence results in a systematic overestimation of person flows.

The two equations (28a) and (28b) are easily seen to be equivalent to the single equation

$$\text{Flow}^{\text{pop}}(x^r, x^p, h) = \text{Flow}^{\text{dev}}(x^r, x^p, h) \cdot \frac{\text{Pop}(x^r)}{\text{Flow}_{\text{out}}^{\text{dev}}(x^r, h)}. \quad (29)$$

Written in this way all known variables are present on the right hand side, while the variable on the left hand side is the one we wish to compute. The factor calibrating the estimate  $\text{Flow}^{\text{dev}}(x^r, x^p, h)$  of a number of devices to the estimate  $\text{Flow}^{\text{pop}}(x^r, x^p, h)$  of a number of persons is hence defined to be the fraction

$$\frac{\text{Pop}(x^r)}{\text{Flow}_{\text{out}}^{\text{dev}}(x^r, h)} \quad (30)$$

and it is independent of the place of presence  $x^p$ . Note, moreover, that this calibration method does not require the actual figures in the flow cube of devices, but only the fractions on the right-hand side of eq. (28a) which are derived from this cube.

## 4.2 Example of calibration

This calibration method is best illustrated via an example. Suppose the Netherlands is partitioned into three regions A, B and C, having residential population figures according to the PRD  $\text{Pop}(A) = 5\,000$ ,  $\text{Pop}(B) = 750$  and  $\text{Pop}(C) = 1\,000$ , respectively. Fix an hour  $h$  and suppose that the corresponding 2-dimensional slice  $\text{Flow}^{\text{dev}}(\cdot, \cdot, h)$  of the flow cube of devices looks as in Table 4.1. This table for example tells us that  $\text{Flow}^{\text{dev}}(A, B, h) = 20$ . We also added the column totals to this table, that is, the incoming flow  $\text{Flow}_{\text{in}}^{\text{dev}}(\cdot, h)$ , and the row totals  $\text{Flow}_{\text{out}}^{\text{dev}}(\cdot, h)$  for each of the regions A, B and C.

**Table 4.1 The slice  $\text{Flow}^{\text{dev}}(\cdot, \cdot, h)$  at hour  $h$  of the flow cube of devices**

		Place of presence			Total
		A	B	C	
Place of residence	A	900	20	80	1 000
	B	80	120	50	250
	C	70	40	140	250
Total		1 050	180	270	

The residential population figures  $\text{Pop}(\cdot)$  for the regions are higher than the row totals, by factors 5, 3 and 4, respectively. Correcting for this discrepancy via our method implies that the rows of the table above should be multiplied by these calibration factors. We then obtain the slice  $\text{Flow}^{\text{pop}}(\cdot, \cdot, h)$  at hour  $h$  of the flow cube of persons as in Table 4.2. The row totals now equal the residential population figures  $\text{Pop}(\cdot)$  and the column totals are the incoming flows of persons  $\text{Flow}_{\text{in}}^{\text{pop}}(\cdot, h)$ .

**Table 4.2 The slice  $\text{Flow}^{\text{pop}}(\cdot, \cdot, h)$  at hour  $h$  of the flow cube of persons**

		Place of presence			Total
		A	B	C	
Place of residence	A	4 500	100	400	5 000
	B	240	360	150	750
	C	350	120	560	1 000
Total		5 090	580	1 110	

# 5 Results

With the methodology explained in Sections 2 to 4 flow cubes of persons can be produced. The low technical complexity of the methods allow for efficient data processing with standard computational resources, but obvious questions about the quality of the output arise due to the simplifying assumptions that have been made. In this section several cubes produced by SN are evaluated for plausibility by checking which natural, known phenomena and events can or cannot be observed. The cube will be evaluated for plausibility by checking which natural, known phenomena and events can or cannot be observed. This report does not aim to further quantify possible errors that have been found, but these results show some of the quality issues that may occur. A major hindrance for a more detailed investigation of errors is the lack of availability of benchmark data against which population flow estimates can be compared. Visualisations were chosen over large data tables as the tool to evaluate the plausibility of the massive amounts of information in flow cubes.

## 5.1 Flow cubes produced

In our discussion up to now  $x$  has stood for a generic administrative region, such as a neighbourhood, district or municipality. The choice for the level of spatial detail at which one is able to produce population flow statistics is restricted by at least the following factors:

- the spatial density of the cells belonging to the MNOs network. This density differs according to, among other factors, the level of urbanicity. Since a mobile network is optimised for the needs of its users, densely populated regions contain more cells to ensure optimal service,
- the accuracy of the model used to estimate the location posterior probabilities  $\mathbb{P}(g | a)$ ,
- the mass lost from the cube by the threshold of 15 devices enforced before export to SN. A greater level of spatial detail namely implies that the cube will contain more cells, each of which is more likely to contain a lower number of devices,
- the market share of the MNO which made the MNO data available.

Consideration of the factors above led SN to construct three flow cubes, all for observation periods five weeks in length:

- one cube which used the uniform prior in the location estimation model, at the level of districts, for the period of 5 March up to and including 8 April 2018,
- two cubes which used the network prior, one at the level of districts and one for municipalities, for the period of 28 May up to and including 1 July 2018.

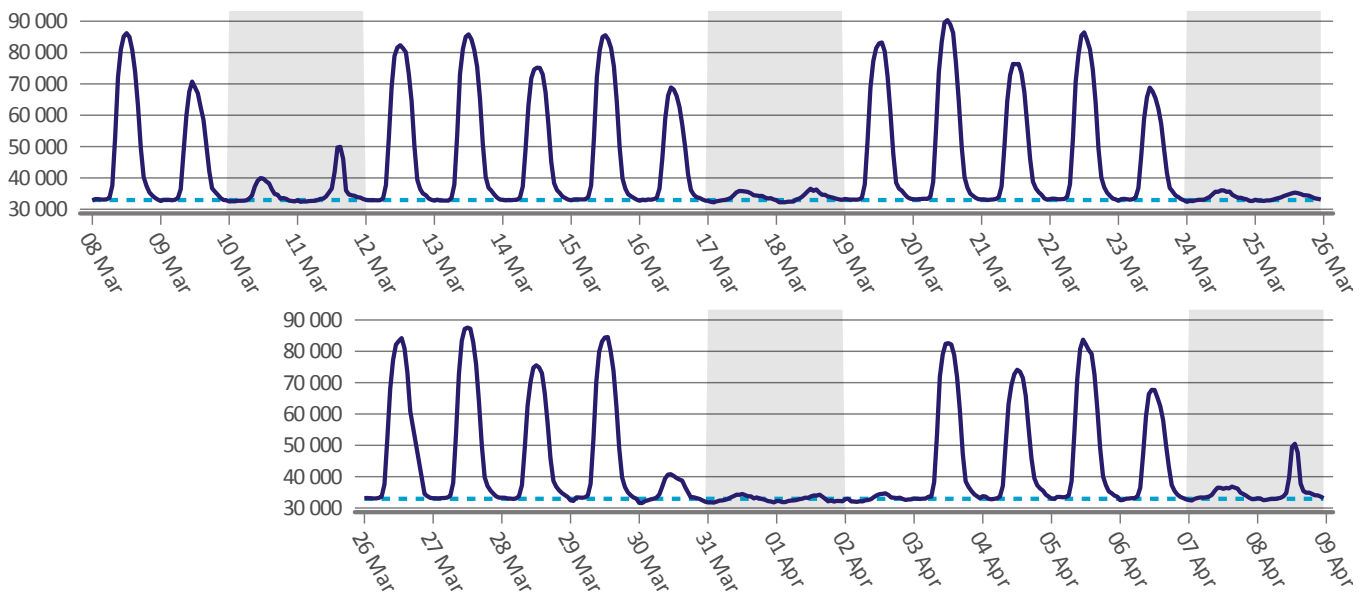
Because for certain durations in the former period the amount of available MNO data was insufficient, the corresponding figures in the flow cube were removed. Consequently, the analysed observation period started on 8 March. The former cube was produced with the uniform instead of the network prior before it was realised that a more advanced prior might be preferable.

## 5.2 Visualisations of flows

Given a fixed region  $x$ , plotting the inflow  $\text{Flow}_{\text{in}}^{\text{pop}}(x, h)$  for varying  $h$  results in the graph of the *population present in  $x$* . This graph shows how the number of residents of the Netherlands present in  $x$  varies over time, in contrast to the residential population of  $x$  which can be approximated to be constant over the short observation periods under consideration.

Figure 5.1 shows a population presence graph of the district East of the municipality of Utrecht, along with the associated dashed, constant residential population graph. Shaded regions indicate weekends. This district is adjacent to the city centre, but stretches to the edge of the city, and includes many shops, the football stadium Galgenwaard and Utrecht Science Park – the largest science park of the Netherlands. It is home to university buildings, a university medical centre and student housing.

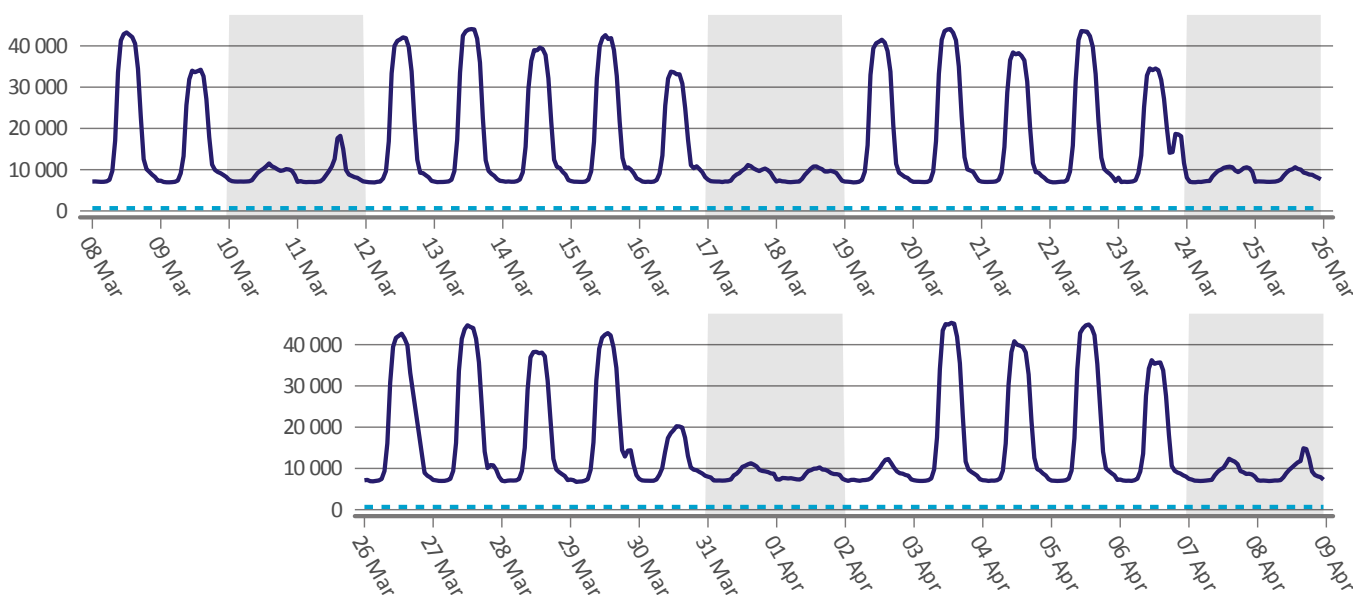
**Figure 5.1 A population presence graph of the district East of the municipality of Utrecht**



The graph shows that the population presence in this district doubles or triples at noon during workweek days with respect to the residential population. Far less people can be observed during weekends. Spikes can be seen, though, on the two Sundays 11 March and 8 April when the football club FC Utrecht played home matches at Galgenwaard. The graph additionally distinguishes Wednesdays and Fridays, on which employees often choose to work fewer hours and universities offer fewer classes. Good Friday fell on 30 March, while 2 April was Easter Monday and Utrecht University and the HU University of Applied Sciences Utrecht were indeed both closed on these dates.

The estimated population presence at night in Utrecht East closely matches the residential population known from the PRD. Our methods do not result in such close matches for all districts, as demonstrated by the population presence graph of the district Amstel III/Bullewijk of Amsterdam shown in Figure 5.2. This district lies on the far outskirts of the city and contains large retail stores, hotels, a university medical centre, the football stadium Johan Cruyff Arena, a concert hall and university examination halls.

**Figure 5.2 A population presence graph of the district Amstel III/Bullewijk of the municipality of Amsterdam**



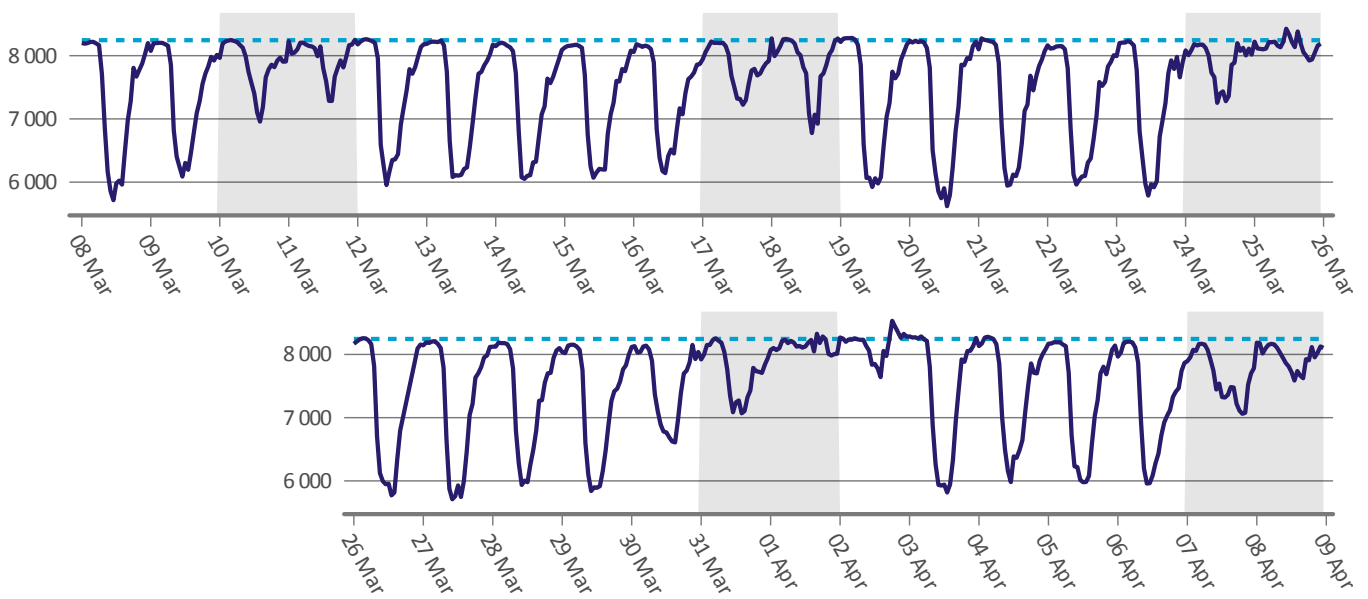
A very similar activity pattern can be observed here as for Utrecht East, including the spikes on 11 March and 8 April when the football club AFC Ajax played home matches at the Arena. However, the residential population of this district was merely 665, while the level of the population presence graph at night is higher with an difference of at least 6 000 people.

In this specific case such a difference can possibly explained by the presence of hotels, adjacent motorways and train and subway stations. There were nevertheless many districts for which we could not interpret such discrepancies. A possible explanation is that the location prior used, or the location estimation model in general, does not sufficiently respect the boundaries of districts. Indeed, while Amstel III/Bullewijk showed a surplus with respect to the residential population, the adjacent districts Holendrecht/Reigersbos and '00' of the municipalities of Amsterdam and Ouder-Amstel, respectively, show deficits. Football matches, being extremely localised in space and time and having well-documented visitor counts, provide additional evidence for this hypothesis. Stadiums in the Netherlands are namely often completely contained within a single district, but they are situated at their boundary. In our analysis it was observed that matches are sometimes not clearly visible in the population presence graph of the stadium's district itself, but they *are* in the neighbouring one.

Figure 5.3 shows a typical population presence graph of a residential area, as a comparison with the districts focused on commerce and education considered so far. Bavel is a village which has been absorbed as a district into the municipality of Breda, but is still slightly geographically separated from it. One observes that the lowest levels of the present population are not reached at night, but at noon, as expected of districts of this type. It should be noted that the population presence graphs of other commuter districts we analysed rarely matched the residential population this cleanly.

June traditionally is a month in which many summer festivals take place throughout the Netherlands. Such events are typically more spread out in space and time than football matches. In the hopes of capturing these well the flow cube for the June period was produced at the municipal level also, and it was simultaneously decided to switch from the uniform to the network prior.

**Figure 5.3 A population presence graph of the district Bavel of the municipality of Breda**



The eight round of the 2018 Grand Prix motorcycle racing season took place on Sunday 1 July 2018 at the TT Circuit in the municipality of Assen. Surrounding events such as qualifying races started on Thursday 27 June, and the preceding TT Festival lasted from the evening of 27 June until the night of Saturday 30 June. These can be clearly read off from the population presence graph of the municipality of Assen shown in Figure 5.4. It should be emphasised that we do not consider the (absolute) level of this graph to be reliable. That is, we do not claim to have measured the number of visitors at the events accurately with the current techniques. Improving the levels of population presence graphs is the subject of ongoing research.

Another example of an observed music festival is *Down the Rabbit Hole*, which took place in 2018 from the morning of Friday 29 June until Sunday night on 1 July, as seen in the population presence graph of the municipality of Beuningen in Figure 5.5. The words of caution we gave about the events in Assen apply here as well.

A dashboard has been published by SN at [SNb] in which the flow cube for the June period at the municipal level can be explored interactively. It features population presence graphs and a population density map, both of which can be animated simultaneously through control buttons. An icon in the upper left-hand corner shows hourly weather information to study the relation with population activities. Furthermore, a municipality can be selected after which the incoming and outgoing flows from and to the other Dutch municipalities are visualised as a fan of arrows. The screenshot in Figure 5.6 shows the (major) origins of the visitors of the *Boulevard Outdoor Festival* in the municipality of Wierden on Saturday 30 June 2018. The number of arrows in such fans is quite small if one expects that the visitors originate from many different municipalities. This is a consequence of the threshold of 15 devices that is enforced on the flow cube of devices before it is exported to SN.

**Figure 5.4 A population presence graph of the municipality of Assen**

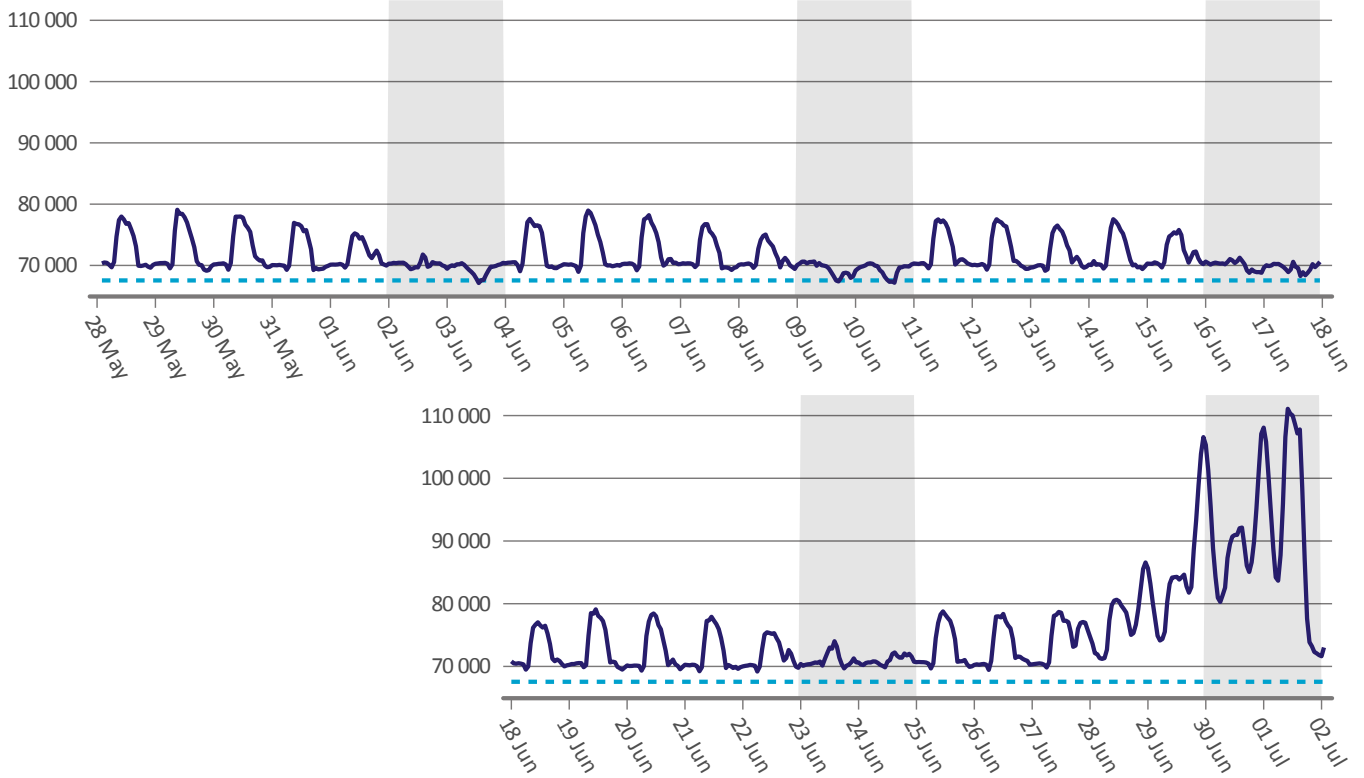


**Figure 5.5 A population presence graph of the municipality of Beuningen**

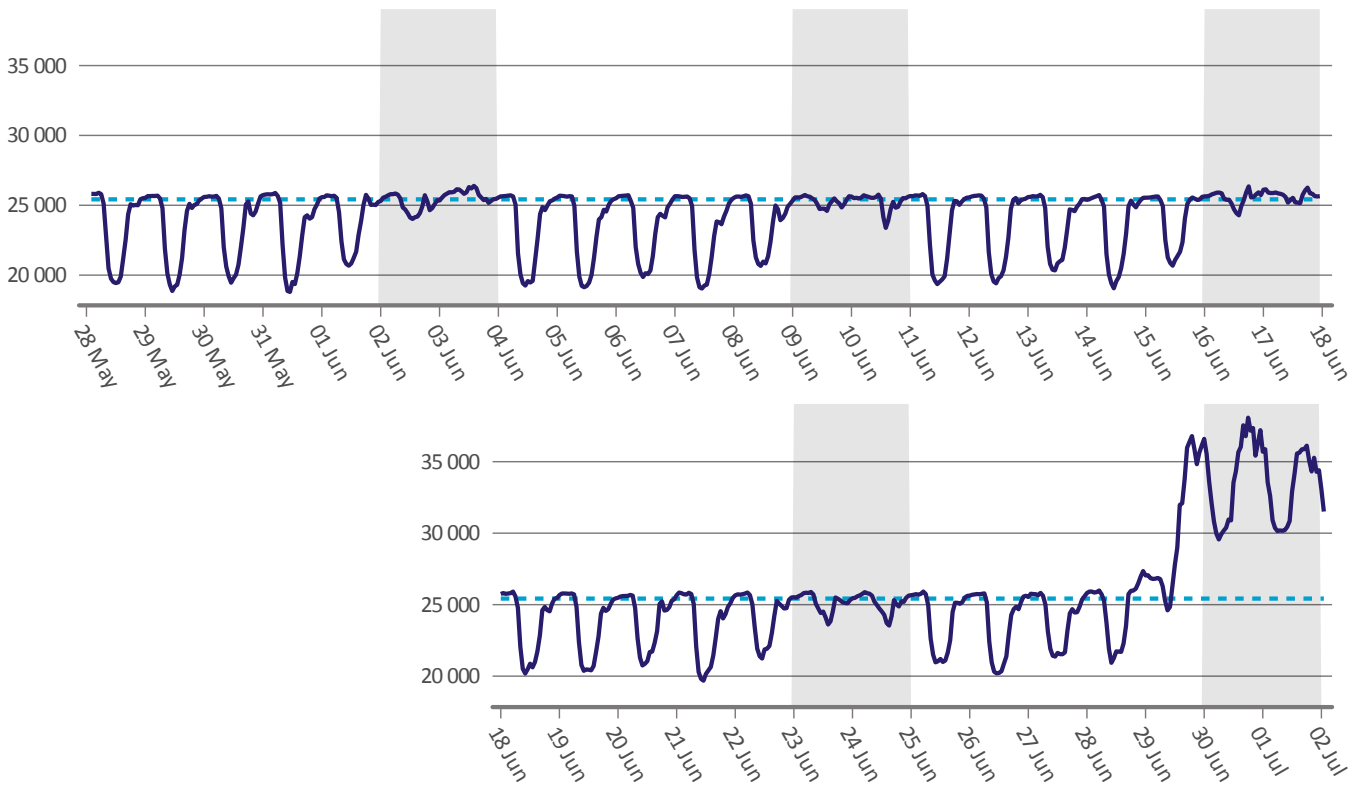
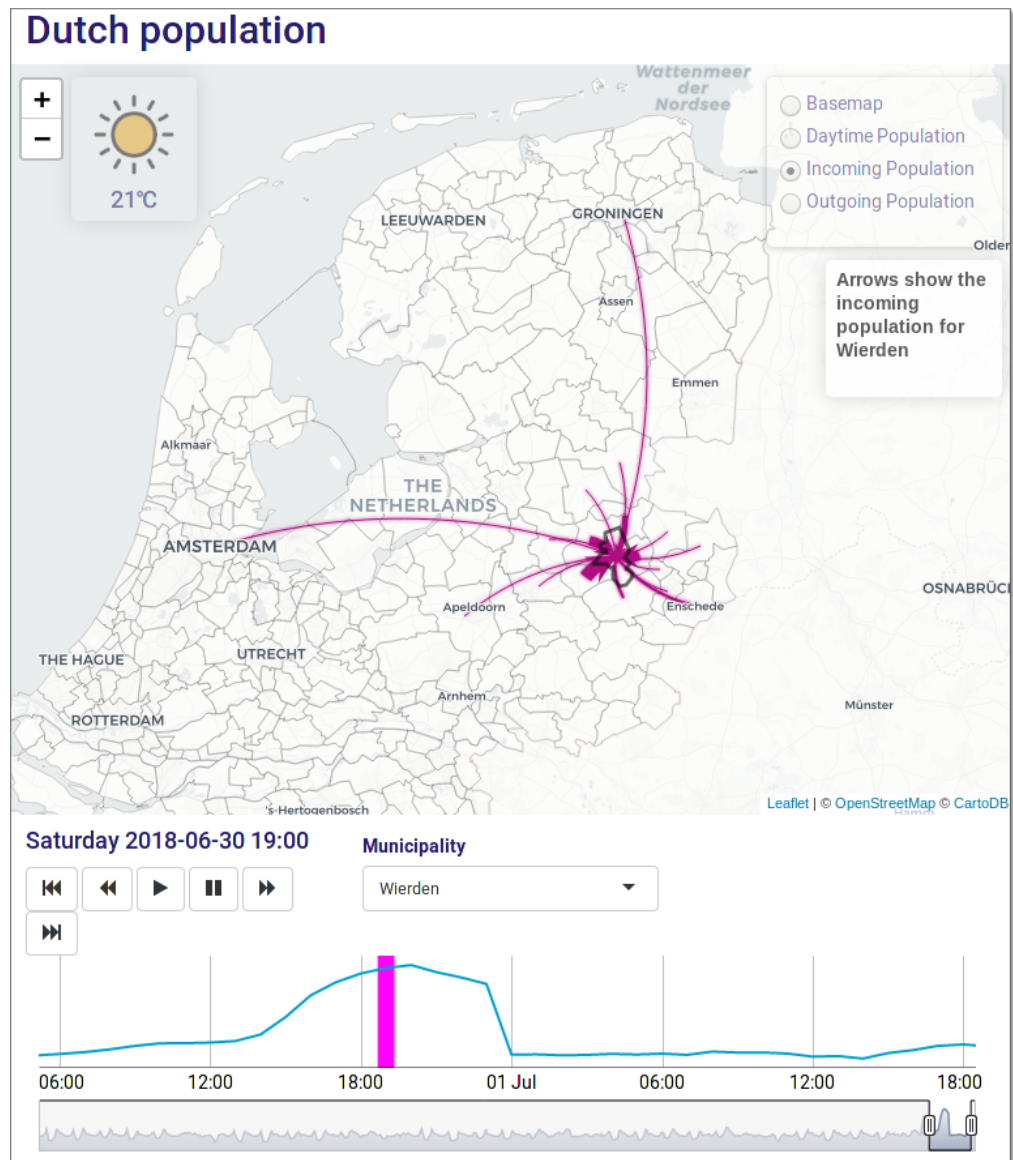


Figure 5.6 A screenshot of the population flow dashboard showing the municipality of Wierden



# 6 Summary and outlook

We have presented a methodology to estimate hourly population flows between Dutch municipalities from aggregated anonymous mobile network operator data. These estimates can be used by policy makers from governmental institutes to analyze mobility among the Dutch population. The results from the pilot study from 2018 have shown that population dynamics can be detected at a high temporal detail: workweek-weekend patterns can be seen, as well as major events.

Section 5 shows that the relatively simple methods developed as part of the ongoing project *Fast Population Statistics* are already able to detect a variety of population activities at a high temporal detail resulting from

- workweeks and weekends,
- (in urban districts) Wednesday and Fridays versus the other days of the workweek,
- holidays, and
- major football matches and festivals.

These activities can be read off by first producing flow cubes of persons and next observing the *relative* changes in the level of population presence graphs and densities of population flow fans.

## 6.1 Methodological improvements

The methodology presented in this report was developed during previous research with actual MNO data. Although we are confident that the results from the methodology will provide key insights for policymakers, we envision some improvements that would be beneficial for quality of the end result. Further research is needed to explore the specifics of these improvements.

We found that the estimates of our present population at night time are not always equal to the registered residential population numbers. Additional auxiliary data could partly solve this issue. For instance, replacing the uniform prior by the network prior in the location estimation model did not seem to improve the spatial blurriness, but in in [TGS20] a *land use prior* is suggested which makes use of administrative data sources on land use to improve the estimated municipality of presence. Another aspect that may help to solve this issue is assigning not one but multiple home cells to a device. A device might switch between different nearby cells even when it remains stationary inside the owner's home.

The current methodology does not take into account Dutch people who are abroad. Auxiliary data, such as the *Continuous Holiday Survey* [SNa], might be used for calibration of the population flow estimates.

The methodology currently assumes that every Dutch residents owns and uses exactly one mobile phone. In reality, there are many people who do not own a mobile phone, in particular young children and elderly people. Furthermore, there are many people who own multiple phones, e.g. one for private and one for business use. Further research is needed to incorporate this.

Finally, it is assumed that every Dutch resident actually lives at address of residence as registered in the PRD. For instance, students in higher education sometimes live in or near the municipality where they study, but are registered at their parents' address. Auxiliary data is needed to compensate for this issue.

At a European level, statistical agencies are collaborating to generate general methodology to use MNO data for official statistics. This work is organized by the European Statistical System hosted by Eurostat (European Commission). The main result so far is that a framework has been introduced in which the whole methodological process to use MNO data to create official statistics is embedded [Ric+20]. While the methodology in this report has not been explicitly designed with this framework in mind, the flowchart in Figure 1.1 can be viewed through this lens.

## 6.2 Further organisation of methodology

# References

- [Cal+11] Francesco Calabrese, Giusy Di Lorenzo, Liang Liu and Carlo Ratti. ‘Estimating origin-destination flows using mobile phone location data’. In: *IEEE Pervasive Computing* 10.4 (Oct. 2011), pp. 36–44.
- [Che+16] Cynthia Chen, Jingtao Ma, Yusak Susilo, Yu Liu and Menglin Wang. ‘The promises of big data and small data for travel behavior (aka human mobility) analysis’. In: *Transportation Research Part C: Emerging Technologies* 68 (July 2016), pp. 285–299.
- [FF10] João Figueiras and Simone Frattasi. *Mobile positioning and tracking: From conventional to cooperative techniques*. John Wiley and Sons, Ltd., 2010.
- [Kor+16] Ahmed D. Kora, Brice A. Elono Ongbwa, Jean-Pierre Cances and Vahid Meghdadi. ‘Accurate Radio Coverage Assessment Methods Investigation for 3G/4G Networks’. In: *Computer Networks* 107 (9th Oct. 2016), pp. 246–257. ISSN: 1389-1286.
- [PDOK] *Dataset: Actueel Hoogtebestand Nederland (AHN1)*. Dutch. Publieke Dienstverlening Op de Kaart (PDOK). URL: <https://www.pdok.nl/introductie/-/article/actueel-hoogtebestand-nederland-ahn1-> (visited on 12th Dec. 2019).
- [Pri17] Kees Prins. *Population register data, basis for the Netherlands Population Statistics*. Statistics Netherlands, 2017. URL: [https://www.cbs.nl/-/media/\\_pdf/2017/38/population-register-data.pdf](https://www.cbs.nl/-/media/_pdf/2017/38/population-register-data.pdf) (visited on 17th Oct. 2019).
- [Ric+20] Fabio Ricciato, Giampaolo Lanzieri, Albrecht Wirthmann and Gerdy Seynaeve. ‘Towards a methodological framework for estimating present population density from mobile network operator data’. In: *Pervasive and Mobile Computing* 68 (2020), p. 101263.
- [SH09] S. Srinivasa and M. Haenggi. ‘Path loss exponent estimation in large wireless networks’. In: *2009 Information Theory and Applications Workshop*. Feb. 2009, pp. 124–129.
- [SNa] *Continu Vakantie Onderzoek (CVO), vanaf 2017*. Dutch. Statistics Netherlands. URL: <https://www.cbs.nl/nl-nl/onze-diensten/methoden/onderzoeksomschrijvingen/korte-onderzoeksbeschrijvingen/continu-vakantie-onderzoek--cvo---vanaf-2017> (visited on 17th Oct. 2019).
- [SNb] *Dutch population*. Statistics Netherlands. URL: <https://dashboards.cbs.nl/v1/dtp/> (visited on 13th Dec. 2019).
- [SNC] *Kerncijfers wijken en buurten 2017*. Dutch. Statistics Netherlands. URL: <https://www.cbs.nl/nl-nl/maatwerk/2017/31/kerncijfers-wijken-en-buurten-2017> (visited on 14th Oct. 2019).
- [SNd] *Onderzoek Verplaatsingen in Nederland (OVIN)*. Dutch. Statistics Netherlands. URL: <https://www.cbs.nl/nl-nl/onze-diensten/methoden/onderzoeksomschrijvingen/korte-onderzoeksbeschrijvingen/onderzoek-verplaatsingen-in-nederland--ovin--> (visited on 17th Oct. 2019).
- [SNe] *Wijk- en buurtkaart 2017*. Dutch. Statistics Netherlands. URL: <https://www.cbs.nl/nl-nl/dossier/nederland-regionaal/geografische-data/wijk-en-buurtkaart-2017> (visited on 18th Oct. 2019).
- [TGS20] Martijn Tennekes, Yvonne A.P.M. Gootzen and Shan H. Shah. *A Bayesian approach to location estimation of mobile devices from mobile network operator data*. Center for Big Data Statistics. May 2020. URL: <https://www.cbs.nl/en-gb/background/2020/22/geographic-location-estimation-of-mobile-devices> (visited on 24th June 2020).

[Val+19] Johan van der Valk, Martijn Souren, Martijn Tennekes, Shan Shah, May Offermans, Edwin de Jonge, Jan van der Laan, Yvonne Gootzen, Sander Scholtus and Anna Mitriaieva. 'Experiences of using anonymized aggregated mobile phone data in The Netherlands'. In: *City data from LFs and Big Data*. European Commission, 28th Feb. 2019. URL: [https://ec.europa.eu/regional\\_policy/en/information/publications/studies/2019/city-data-from-lfs-and-big-data](https://ec.europa.eu/regional_policy/en/information/publications/studies/2019/city-data-from-lfs-and-big-data) (visited on 17th Oct. 2019).

## Colophon

*Publisher*

Statistics Netherlands  
Henri Faasdreef 312, 2492 JP The Hague  
[www.cbs.nl](http://www.cbs.nl)

*Prepress*

Statistics Netherlands

*Design*

Edenspiekermann

*Enquiries*

Telephone: +31 88 570 70 70  
Via contact form: [www.cbs.nl/infoservice](http://www.cbs.nl/infoservice)

© Statistics Netherlands, The Hague/Heerlen/Bonaire 2020.  
Reproduction is permitted, provided Statistics Netherlands is quoted as the source.